# Comparison of Lamina Cribrosa Morphology in Eyes with Ocular Hypertension and Normal-Tension Glaucoma

Ji-Ah Kim,[1] Tae-Woo Kim,[1] Eun Ji Lee,[1] Michaël J. A. Girard,[2,3] and Jean Martial Mari[4]

[1]Department of Ophthalmology, Seoul National University College of Medicine, Seoul National University Bundang Hospital, Seongnam, Korea
[2]Department of Biomedical Engineering, National University of Singapore, Singapore
[3]Singapore Eye Research Institute, Singapore National Eye Centre, Singapore
[4]GePaSud, Université de la Polynésie Française, Tahiti, French Polynesia

Correspondence: Tae-Woo Kim, Department of Ophthalmology, Seoul National University College of Medicine, Seoul National University Bundang Hospital, 82, Gumi-ro, 173 Beon-gil, Bundang-gu, Seongnam, Gyeonggi-do 463-707, Korea; twkim7@snu.ac.kr.

**Received:** May 8, 2019
**Accepted:** January 29, 2020
**Published:** April 9, 2020

Citation: Kim J-A, Kim T-W, Lee EJ, Girard MJA, Mari JM. Comparison of lamina cribrosa morphology in eyes with ocular hypertension and normal-tension glaucoma. *Invest Ophthalmol Vis Sci.* 2020;61(4):4. https://doi.org/10.1167/iovs.61.4.4

**Purpose.** To characterize differences in the lamina cribrosa (LC) morphology between healthy, ocular hypertension (OHT), and naive normal-tension glaucoma (NTG) eyes.

**Methods.** Each group consisted of 80 eyes of 80 participants who were matched for age, sex, and axial length. The participants underwent enhanced-depth-imaging volume scanning of the optic nerve head using spectral-domain optical coherence tomography. The lamina cribrosa curvature index (LCCI) and lamina cribrosa thickness (LCT) were measured in horizontal B-scan images spaced equidistantly across the vertical diameter of the optic disc.

**Results.** The LCCIs in all seven planes were smaller in both OHT and healthy eyes than in NTG eyes (all $P < 0.001$), and did not differ significantly between the OHT and healthy eyes. The LCTs in all three planes were greatest in OHT eyes followed by healthy and then NTG eyes (all $P < 0.001$). Overall, the larger LCCI was associated with smaller LCT ($P < 0.001$).

**Conclusions.** The LC was thin and steeply curved in NTG eyes than in healthy and OHT eyes. In OHT eyes, the LC was thick, and its curvature was comparable to healthy eyes. Longitudinal studies are required to examine whether the straight and thickened LCs in OHT eyes precede the onset of OHT or are a protective response to elevated intraocular pressure.

Keywords: ocular hypertension, normal-tension glaucoma, lamina cribrosa

Glaucoma is a leading cause of irreversible blindness worldwide. Elevated intraocular pressure (IOP) has been regarded as the most important risk factor for glaucoma development.[1–3] However, more than half of glaucoma patients have untreated IOPs within the normal range, being diagnosed with so-called normal-tension glaucoma (NTG).[4,5] In addition, 90.5% of patients with untreated ocular hypertension (OHT) did not develop glaucoma over a 5-year follow-up period.[6] These findings raise questions concerning the mechanism by which IOP contributes to the pathophysiology of glaucomatous optic neuropathy (GON).

Posterior deformation of the lamina cribrosa (LC) is thought to play an intermediary role in the development of optic nerve damage induced by IOP-related stress.[7–13] A study employing an experimental glaucoma model induced by elevated IOP found that LC deformation occurs prior to a detectable loss of the retinal nerve fiber layer (RNFL).[12] In contrast, posterior LC deformation was not observed in an optic-nerve-crush model, despite substantial loss of RNFL.[14] These findings suggest that posterior LC deformation is induced by IOP-related stress rather than being secondary to axonal loss. Because optic nerve axons pass through the LC pores, LC deformation may impose stress and insult on these axons, ultimately leading to the death of retinal ganglion cells through various mechanisms, including blockade of axonal transport.[15,16] Based on the understanding that posterior LC deformation plays a central role in the development of glaucoma and is not determined solely by IOP, we hypothesized that the LC evaluation may provide a clue that may explain the discordance between IOP and the occurrence of glaucoma, as illustrated by eyes with NTG and OHT. In this regard, it is worthy to note that OHT eyes have thicker LC than healthy eyes.[17] Thicker LC may be more resistant to IOP-induced stress, thereby being less deformed at the same level of IOP-induced stress. Meanwhile, glaucoma animal model studies have demonstrated that LC was thicker in eyes with elevated IOP compared with the fellow control eyes.[10,18] A later study demonstrated that the LC thickness difference between the eyes with elevated IOP and the fellow control eyes was greater than the physiologic intereye difference defined from healthy monkeys.[19] The findings suggest the possibility that thicker LC may be a response to elevation of IOP. Without longitudinal study, it cannot be confirmed whether thickened LC is prior to IOP

elevation or have become thickened in response to it. None the less, comparison of LC morphology, including its thickness and shape between OHT and NTG eyes, may provide additional insight into the discordance between IOP and occurrence of glaucoma. This study therefore assessed differences in LC morphology between OHT and naive NTG eyes and compared these eyes with healthy control eyes.

## Methods

This investigation was a component of the ongoing prospective Investigating Glaucoma Progression Study involving glaucoma, glaucoma suspect, and healthy subjects at the Glaucoma Clinic of Seoul National University Bundang Hospital. The study included consecutive subjects who met the eligibility criteria. Each patient provided written informed consent to participate. This study was approved by the institutional review board of Seoul National University Bundang Hospital and adhered to the tenets of the Declaration of Helsinki.

### Study Subjects

Each participant underwent comprehensive ophthalmic examinations, including visual acuity and refractive error assessment, slit-lamp biomicroscopy, Goldmann applanation tonometry, gonioscopy, dilated stereoscopic examination of the optic disc, stereo disc photography, and red-free fundus photography (Kowa VX-10; Kowa Medicals, Torrance, CA, USA). Other ophthalmic examinations included scanning of the circumpapillary RNFL and the optic nerve head (ONH) using spectral-domain (SD) optical coherence tomography (OCT) (Spectralis OCT; Heidelberg Engineering, Heidelberg, Germany), and standard automated perimetry (Humphrey Field Analyzer II 750 and 24-2 Swedish interactive threshold algorithm; Carl Zeiss Meditec, Dublin, CA, USA). Subjects also underwent measurements of the corneal curvature (KR-1800; Topcon, Tokyo, Japan), central corneal thickness (CCT) (Orbscan II; Bausch & Lomb Surgical, Rochester, NY, USA), and axial length (AXL) (IOLMaster version 5; Carl Zeiss Meditec).

Subjects in the three groups were 1:1:1 matched by age, sex, and AXL. Participants underwent IOP measurement and optic disc scanning using enhanced depth imaging (EDI) SD-OCT in the baseline examination, which was performed prior to initiating ocular hypotensive treatment. The measured IOP was corrected for its dependence on the CCT. Definition of NTG, OHT, and healthy subjects, criteria for inclusion and exclusion, and the measurement and correction of IOP are described in the Appendix in the Supplementary material.

### Measurement of LC Curvature Index and LC Thickness

The ONH was imaged using the EDI technique of the Spectralis OCT system.[20] The detailed description of EDI-OCT of the optic disc is found in the Appendix in the Supplementary material.

We quantified the posterior bowing of the LC on the SD-OCT B-scan images after adaptive compensation,[21–23] by assessing the lamina cribrosa curvature index (LCCI) as the degree of inflection of a curve representing a section of the LC. The method used to measure the LCCI has been described previously[24–27] and is found in the Appendix in the Supplementary material. In brief, the LCCI was determined by first measuring the width of Bruch's membrane opening (BMO) ($W$) and then measuring the LC curvature depth (LCCD) within the BMO in each B-scan (Supplementary Fig. S1D). The LCCI was then calculated as (LCCD/$W$) $\times$ 100. The measurements made in the seven B-scans were used to calculate the mean LCCI of the eye.

Thin-slab maximum intensity projection (MIP) image was used to measure lamina cribrosa thickness (LCT) because it allows detection of a straighter posterior LC border.[28] The technique of generating thin-slab MIP images is described in the Appendix in the Supplementary material. The LCT was measured as the distance between the anterior and posterior borders at the central 3 points (center of the BMO reference line, and 2 additional points 100 and 200 µm apart from the center point to temporal direction) in each MIP thin-slab image in the direction perpendicular to the BMO reference line at the measurement point (Supplementary Fig. S1E). The measurements made in the three points were used to calculate the mean LCT of the slab. The measurements obtained from the three planes were used to calculate the mean LCT of the eye.

The LCCI and LCT were measured using a manual caliper tool in Amira software (Amira 5.2.2; Visage Imaging, Berlin, Germany) by two experienced observers (J-AK and EJL) who were masked to the clinical information. The mean of the measurements made by the two observers was used for the analysis.

### Data Analyses

The interobserver agreements for the LC measurements were assessed by calculating intraclass correlation coefficients (ICCs). Comparisons between groups were performed using analysis of variance with the post hoc Scheffé test for continuous variables and the Kruskal–Wallis test for categorical variables, and raw data were subjected to Bonferroni correction on the basis of the number of comparisons in each analysis. Regression analyses were performed to investigate the factors associated with the mean LCCI. Data are presented as mean $\pm$ standard deviation values except where indicated otherwise. All analyses were performed by using SPSS version 22.0 (IBM Corporation, Armonk, NY, USA). $P$ values $<0.05$ were considered to indicate statistical significance.

## Results

### Subject Clinical Demographics

This cross-sectional study initially involved 252 healthy, 105 OHT, and 231 naive NTG subjects, among whom 41 healthy, 19 OHT, and 67 NTG subjects were excluded because of the presence of a tilted or torted disc. Twenty-one subjects were further excluded because image quality of the scans was too low to allow either the anterior or posterior border of the LC to be delineated clearly, leaving 191 healthy, 82 OHT, and 167 NTG subjects. After matching for age, sex, and AXL, each group consisted of 80 eyes of 80 subjects (a total of 240 eyes).

Table 1 summarizes the clinical characteristics of included subjects. The measured and corrected IOPs at the time of EDI-OCT were highest in OHT eyes followed by NTG and healthy eyes ($P < 0.001$). The CCT was larger in OHT eyes

Investigative Ophthalmology & Visual Science

**Table 1.** Clinical Characteristics of OHT, NTG, and Healthy Eye

| Variables | OHT (A) ($n$ = 80) | NTG (B) ($n$ = 80) | Healthy (C) ($n$ = 80) | $P$ Value* | Post Hoc† |
|---|---|---|---|---|---|
| Age, y | 53.8 ± 12.6 | 52.9 ± 13.0 | 52.7 ± 13.3 | 0.864 | |
| Male, $n$ (%) | 33 (41.3) | 33 (41.3) | 33 (41.3) | 1.000 | |
| CCT, µm | 579.8 ± 35.2 | 547.0 ± 33.6 | 551.4 ± 36.0 | **0.001** | B=C<A |
| AXL, mm | 24.14 ± 1.47 | 24.03 ± 1.10 | 24.0 ± 1.17 | 0.744 | |
| Spherical equivalent, diopters | –0.78 ± 2.44 | –0.74 ± 2.00 | –0.52 ± 2.01 | 0.719 | |
| Measured IOP‡, mm Hg | 24.7 ± 2.3 | 13.8 ± 2.3 | 12.9 ± 2.2 | **<0.001** | C<B<A |
| Corrected IOP, mm Hg | 23.9 ± 2.3 | 14.8 ± 2.3 | 13.2 ± 2.4 | **<0.001** | C<B<A |
| Global RNFL thickness, µm | 98.4 ± 8.9 | 78.2 ± 12.3 | 98.7 ± 9.2 | **<0.001** | B<A=C |
| BMO area, mm$^2$ | 2.31 ± 0.40 | 2.32 ± 0.36 | 2.38 ± 0.41 | 0.458 | |
| Visual field mean deviation, dB | –0.05 ± 0.82 | –4.55 ± 3.94 | –0.05 ± 0.77 | **<0.001** | B<A=C |
| Mean $W$, µm | 1394.68 ± 164.29 | 1387.79 ± 173.55 | 1441.22 ± 181.12 | 0.107 | |
| Disc ovality | 0.91 ± 0.08 | 0.91 ± 0.07 | 0.91 ± 0.06 | 0.935 | |
| Cup/disc ratio | 0.43 ± 0.14 | 0.73 ± 0.05 | 0.42 ± 0.12 | **<0.001** | A=C<B |
| SBP, mm Hg | 128.4 ± 14.4 | 126.1 ± 13.4 | 124.6 ± 13.0 | 0.237 | |
| DBP, mm Hg | 76.2 ± 10.0 | 75.5 ± 8.4 | 74.5 ± 9.7 | 0.533 | |
| Self-reported diabetes, $n$ (%) | 13 (16.3) | 5 (6.3) | 8 (10.0) | 0.121 | |
| Self-reported hypertension, $n$ (%) | 26 (32.5) | 24 (30.0) | 20 (25.0) | 0.569 | |
| Family history of glaucoma, $n$ (%) | 7 (8.8) | 4 (5.0) | 7 (8.8) | 0.582 | |
| Migraine, $n$ (%) | 8 (10.0) | 10 (12.5) | 10 (12.5) | 0.851 | |
| Cold extremities, $n$ (%) | 14 (17.5) | 14 (17.5) | 16 (20.0) | 0.895 | |

Values are shown in mean ± standard deviation or $n$ (%) values, with statistically significant $P$ values in boldface.

OHT, ocular hypertension; NTG, normal tension glaucoma; CCT, central corneal thickness; AXL, axial length; IOP, intraocular pressure; RNFL, retinal nerve fiber layer; BMO, Bruch's membrane opening; $W$, width of BMO; SBP, systolic blood pressure; DBP, diastolic blood pressure.

* Comparison was performed using ANOVA and Kruskal–Wallis.

† Post hoc analysis was performed using the Scheffé test.

‡ Untreated IOP for NTG eyes.

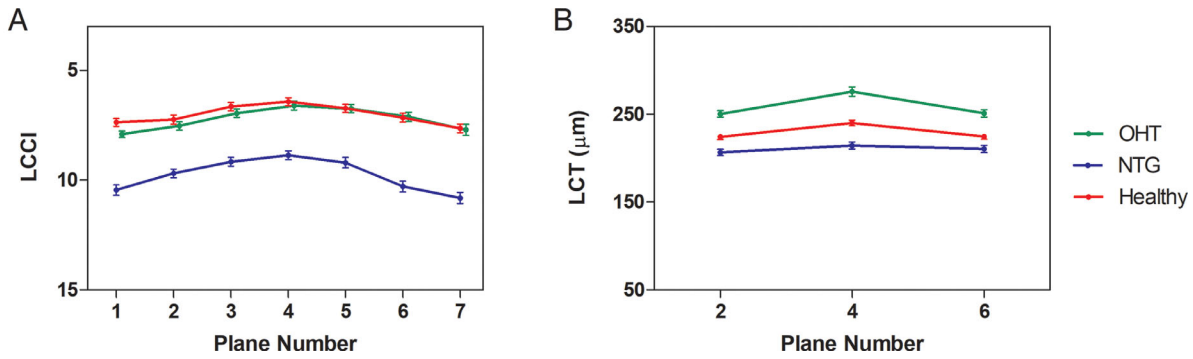


**Figure 1.** LCCI (**A**) and LCT (**B**) profiles in seven and three horizontal B-scans in OHT, NTG, and healthy eyes. *Error bars* represent SEM. (**A**) The LCCI was significantly larger in NTG than in healthy and OHT eyes in all seven planes (all $P < 0.001$). (**B**) The LCT was greatest in OHT eyes followed by healthy and then NTG eyes in all three planes (all $P < 0.001$).

than in NTG and healthy eyes ($P = 0.001$). Cup/disc ratio was larger in NTG eyes than in OHT and healthy eyes, whereas the global RNFL thickness and mean deviation of visual field test were smaller in NTG eyes than in OHT and healthy eyes (all $P < 0.001$).

## Differences in LCCI and LCT Among OHT, NTG, and Healthy Eyes

The measurement of the LCCI and LCT showed excellent intraobserver reproducibility (ICC = 0.960 and 0.924, respectively; 95% confidence interval = 0.948–0.969 and 0.902–0.941, respectively). Figure 1 shows the measured LCCI and LCT values in each group. The LCCIs in all seven measured planes were larger in NTG eyes than in OHT and healthy eyes (all $P < 0.001$; Table 2, Fig. 1A), and did not differ significantly between healthy and OHT eyes. The LCT was greatest in OHT eyes, followed by healthy and then NTG eyes (all $P < 0.001$; Table 3, Fig. 1B). Figure 2 illustrates representative cases matched by age, sex, and AXL, which shows that the LC curvature and LCT were greatest in the NTG and OHT eyes, respectively.

## Factors Influencing LCCI

Overall, the larger LCCI was associated with smaller LCT ($P < 0.001$; Fig. 3, Supplementary Table S1). In the OHT eyes, smaller AXL ($P \leq 0.006$), higher measured IOP ($P \leq 0.008$), and corrected IOP ($P \leq 0.027$) were associated with a larger average LCCI in both univariate and multivariate analyses (Supplementary Table S2). In the NTG eyes, both univariate and multivariate analyses indicated that only higher measured IOP ($P \leq 0.034$) and corrected IOP ($P < 0.001$) were associated with a larger average LCCI

**Table 2.** Comparison of LCCI Between OHT, NTG, and Healthy Eyes

| Plane no. | OHT (A) ($n$ = 80) | NTG (B) ($n$ = 80) | Healthy (C) ($n$ = 80) | $P$ Value* | Post Hoc† |
|---|---|---|---|---|---|
| 1 | 7.92 ± 1.33 | 10.46 ± 2.11 | 7.38 ± 1.59 | **<0.001** | A=C<B |
| 2 | 7.54 ± 1.71 | 9.70 ± 1.73 | 7.25 ± 1.95 | **<0.001** | A=C<B |
| 3 | 6.96 ± 1.71 | 9.17 ± 1.74 | 6.66 ± 1.75 | **<0.001** | A=C<B |
| 4 | 6.61 ± 1.81 | 8.88 ± 1.82 | 6.44 ± 1.61 | **<0.001** | A=C<B |
| 5 | 6.75 ± 1.63 | 9.21 ± 2.06 | 6.73 ± 1.62 | **<0.001** | A=C<B |
| 6 | 7.12 ± 1.86 | 10.30 ± 2.22 | 7.17 ± 1.79 | **<0.001** | A=C<B |
| 7 | 7.72 ± 2.27 | 10.82 ± 2.24 | 7.65 ± 1.77 | **<0.001** | A=C<B |
| Average | 7.24 ± 1.29 | 9.79 ± 1.36 | 7.04 ± 1.31 | **<0.001** | A=C<B |

Values are shown in mean ± standard deviation, with statistically significant $P$ values in boldface.

* Comparison was performed using ANOVA. Bonferroni correction was applied to raw data for measurements in the seven locations. Values that were significant after Bonferroni correction ($P < 0.007$; 0.05/7) are shown in bold.

† Post hoc analysis was performed using the Scheffé test.

**Table 3.** Comparison of LCT between OHT, NTG, and Healthy Eyes

| Plane no. | OHT (A) ($n$ = 80) | NTG (B) ($n$ = 80) | Healthy (C) ($n$ = 80) | $P$ Value* | Post Hoc† |
|---|---|---|---|---|---|
| 2 | 250.4 ± 32.6 | 206.6 ± 30.8 | 224.3 ± 25.7 | **<0.001** | B<C<A |
| 4 | 275.9 ± 47.5 | 214.5 ± 35.9 | 240.0 ± 29.0 | **<0.001** | B<C<A |
| 6 | 251.0 ± 36.5 | 210.6 ± 37.2 | 224.6 ± 25.6 | **<0.001** | B<C<A |
| Average | 259.1 ± 32.5 | 210.5 ± 30.2 | 229.6 ± 20.3 | **<0.001** | B<C<A |

Values are shown in mean ± standard deviation, with statistically significant $P$ values in boldface.

* Comparison was performed using ANOVA. Bonferroni correction was applied to raw data for measurements in the three locations. Values that were significant after Bonferroni correction ($P < 0.017$; 0.05/3) are shown in bold.

† Post hoc analysis was performed using the Scheffé test.

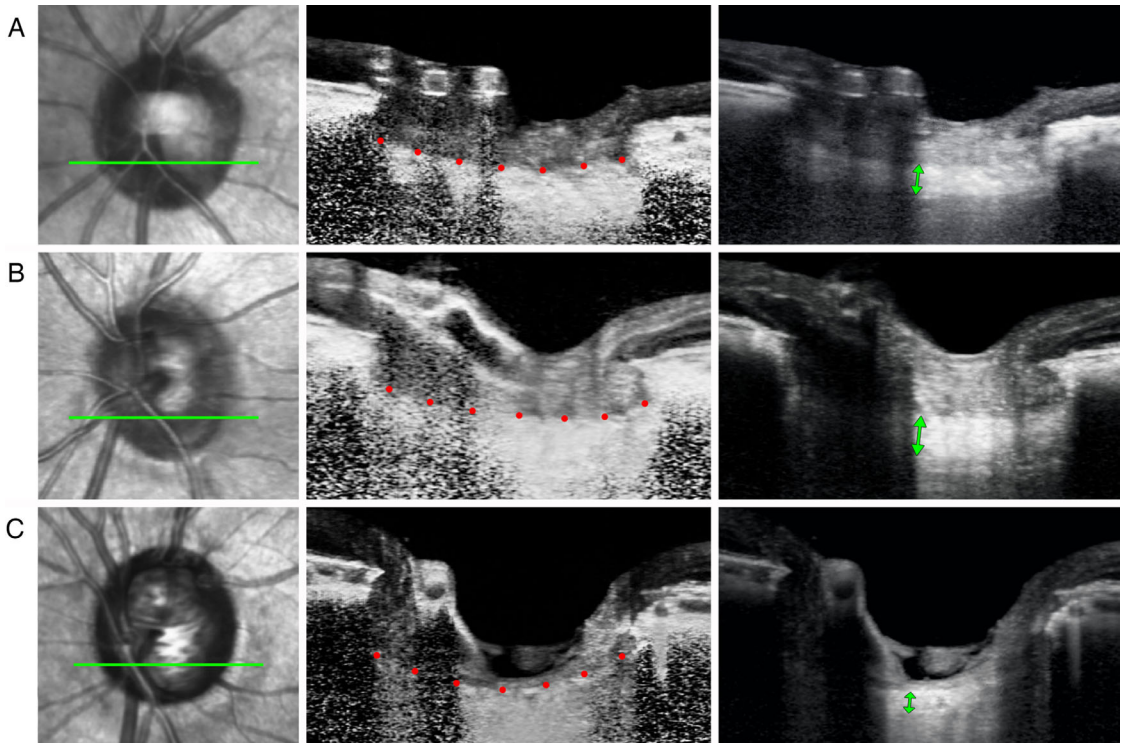


**Figure 2.** Three representative cases. (*Left*) En face images of the left eyes of a 62-year-old man with a healthy eye (**A**), a 60-year-old man with an OHT eye (**B**), and a 62-year-old man with an NTG eye (**C**), respectively. (*Middle*) B-scan images postprocessed using adaptive compensation in the plane indicated by the *green lines* in the en face images. Note that the degree of posterior bowing of the anterior LC surface (*red dots*) was greatest in the NTG eye. (*Right*) MIP images. Note that the LC thickness (*green arrows*) was greatest in the OHT eye and smallest in the NTG eye.

Investigative Ophthalmology & Visual Science

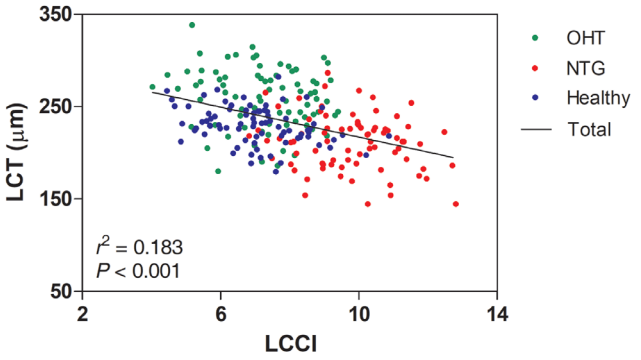


**Figure 3.** Scatter plot showing the relationship between the LCCI and the LCT. Overall, the larger LCCI was associated with smaller LCT ($P < 0.001$) (*solid line*).

(Supplementary Table S3). In healthy eyes, higher measured IOP ($P = 0.001$) and corrected IOP ($P = 0.021$), smaller AXL ($P = 0.002$), and smaller LCT ($P = 0.003$) were associated with a larger average LCCI in the univariate analysis. In the multivariate analysis, smaller AXL ($P = 0.005$), smaller LCT ($P \leq 0.050$), and higher measured IOP ($P = 0.001$) and corrected IOP ($P = 0.009$) were associated with a larger LCCI (Supplementary Table S4).

## Discussion

The present cross-sectional study found that the LCCI was greater in NTG than in OHT eyes and the LCT was significantly smaller in NTG than in OHT eyes. To our knowledge, this study is the first to compare the LC morphology between the OHT and NTG eyes.

The finding that the LC is less curved in OHT than in NTG eyes is especially interesting, as IOP was higher in the former. This finding raises the possibility that LC bowing occurs secondary to axonal loss. However, this possibility is not likely, as LC deformation was found to occur prior to a detectable loss of the RNFL in experimental glaucoma model studies induced by IOP elevation.[12,29] In addition, posterior LC deformation was not observed in an optic-nerve-crush model using monkey eyes, despite substantial RNFL loss.[14] Moreover, larger LCCI was recently found to predict a faster rate of RNFL loss in eyes with suspected glaucoma,[26] indicating that a posteriorly curved LC is a leading factor contributing to RNFL damage. However, the possibility that curved LC in NTG eyes is an innate feature cannot be ruled out without a longitudinal study.

The LC was thicker in eyes with OHT. It is possible that OHT patients may have innate thicker LC. Another possibility is that LC was thickened as a response to IOP elevation. Previous experimental studies demonstrated that LC was thicker in eyes with higher IOP.[10,18,19,30] The intereye difference was greater than physiologic intereye difference defined based on the observation in six[19] and four[30] animals. Although those were not a longitudinal observation, the data suggest that LC may be thickened as a remodeling response to IOP elevation.

Both experimental[10,13] and clinical[31] studies showed that the LC curve within an individual is dependent on the IOP. Therefore intergroup differences of LCCI are attributable to a combination of innate interindividual variations and changes over time induced by translaminar pressure difference (TLPD). It is impossible to separate the innate and acquired components of LCCI in an individual. Nevertheless, if a larger LCCI in the NTG group is predominantly because of the innate component, our findings indicate that eyes with posteriorly curved LC are more susceptible to glaucomatous insult, such as IOP-induced stress. Additional studies are warranted to determine whether a more steeply curved LC promotes axonal damage or, more likely, hampers axonal transport at the same level of TLPD. If a larger LCCI reflects a greater degree of acquired LC deformation, the current findings would indicate that glaucomatous axonal damage is not likely to develop without prior LC deformation, even in patients with high IOP. This would support the hypothesis that posterior LC deformation is a principal pathogenic component of GON.

Elevated IOP induces posterior bowing of the LC.[10,13] Conversely, IOP lowering surgery was found to reduce LC curvature.[31] These findings suggest that IOP-induced stress is a primary driving force that generates and sustains LC deformation. Assuming that a larger LCCI reflects greater LC bowing, then it is intriguing how LCCI would be larger in eyes with NTG than OHT. It has been suggested that LC deformation is derived not only by IOP but also by retrolaminar tissue pressure.[32,33] In other words, the TLPD is likely to be more strongly related with LC deformation than IOP. The TLPD may be high in an eye with a low retrolaminar tissue pressure, even if the IOP is within the normal range, resulting in a significantly curved LC. In contrast, OHT patients who do not develop glaucoma may have a higher retrolaminar pressure. Indeed, the Beijing Eye study estimated that the cerebrospinal fluid pressure was elevated in OHT subjects.[34]

Another important factor for determining the degree of LC deformation could be the material properties of the LC, as the LC may be stiffer in eyes with OHT or their collagen fiber arrangements restrict IOP-induced LC deformation.[35] In contrast, the LC may be more flexible in NTG eyes. The present study found that the LCT was significantly greater in OHT eyes and lower in NTG eyes than healthy eyes. This finding is in accord with the Han et al.[17]'s study, which reported thicker LCT in OHT than healthy eyes. It remains to be determined whether the thicker LC in OHT eyes was prior to the elevation of IOP or remodeling response to elevated IOP. In this regard, it is noteworthy that LC was thicker in early glaucoma model eyes induced by IOP elevation compared with the contralateral control eye.[10,18,36] Whichever the case is, a thicker LC would be relatively more resistant to deformation (assuming that the stiffness of each laminar sheet is similar), allowing optic nerve axons to withstand the stress from a higher IOP. According to the Laplace's law, wall stress can be calculated using the equation $\sigma = pr/2t$, where $\sigma$ = wall stress, p = internal pressure, r = radius, and t = thickness. Therefore those with small LCT is related with higher wall stress, resulting in greater LCCI.[37]

Discordance between IOP and the LC configuration may be attributable to the property of the peripapillary sclera. Bellezza et al.[38] reported that the peripapillary scleral change may have important effect on the LC position change according to IOP elevation. Sigal et al.[39] demonstrated the possibility that LC behavior to IOP elevation may be different depending on the relative stiffness/compliance of the peripapillary sclera and LC. According to their model, the LC may move anteriorly in response to IOP elevation in eyes with compliant sclera and stiff LC. It is possible that the OHT eyes have a more compliant sclera than LC.

Investigative Ophthalmology & Visual Science

This may be a congenital or an acquired feature. Experimental studies demonstrated that sclera became hypercompliant in response to acute IOP elevation as in experimental monkey studies.[10,36,40] On the contrary, NTG eyes may have stiff sclera and compliant LC that may facilitate the posterior deformation of the LC.

Whereas the intergroup comparisons showed that LCCI was lower in OHT than in NTG eyes, comparisons within each group showed that LCCI was positively associated with IOP. Although LCCI is not influenced solely by IOP, IOP is an important factor influencing LC morphology. If all other conditions, including LC properties, are equal, LCCI would positively correlate with IOP. In addition, the current study suggests that OHT and NTG eyes may have significant intergroup differences and intragroup similarities in terms of resistance of LC to IOP-related deformation.

The present study had several limitations. First, for precise quantification, a LC surface reference line should be drawn from the LC insertion points. However, the LC is often not visible outside the BMO region. Therefore measurements of LC curvature in the present study included only the LC within the BMO. This limitation, however, likely did not seriously affect the outcome of this study, as the LCCI measured from the entire LC (between the LC insertion points) did not differ significantly from that measured on the LC within the BMO in eyes with an LC visible up to the LC insertion point.[31] Thus the curvature of the LC assessed within the BMO may represent the actual LC curvature. Second, as curvature is a geometric entity, being the inverse of the radius of the arc of a circle that best fits the portion of a curve, the LCCI in the present study does not correspond exactly to the actual LC curvature.[31] Third, eyes with a tilted or torted optic disc were excluded; hence the findings of this study cannot be directly applied to eyes with such conditions. In addition, subjects in the different groups were matched for age, sex, and AXL. Fourth, BMO-minimum rim width, which can be complimentary for detecting structural abnormality in glaucoma, was not used in this study. This was because many of the patients included in the study were enrolled before BMO-minimum rim width protocol became available. However, the RNFL thickness was within normal limit without progressive change for more than 2 years in the OHT group. Therefore it can be deemed that glaucomatous damage was not present in OHT eyes. Conversely, NTG and healthy eyes were defined based on the structural and functional glaucomatous damage. Therefore the possibility that the subjects were misdiagnosed into NTG or healthy eyes may be negligible. Fifth, IOP correction was done only using CCT in this study. Liu and Roberts[41] suggested that differences in corneal biomechanics across individuals may have greater impact on IOP measurement error than corneal thickness. However, there is no established method to correct IOP reflecting individual corneal biomechanical properties. Therefore we used IOP data corrected by CCT together with uncorrected IOP. Finally, of factors conferring resistance to LC deformation, the only parameter measured was LCT. Although LC stiffness is also likely important, there is currently no established method of evaluating LC stiffness.

## Conclusions

The LC was thin and steeply curved in NTG eyes. In contrast, the LC was thick and had a comparable curvature to healthy eyes in OHT eyes. Longitudinal studies are required to examine whether the straight and thickened LCs in human OHT eyes precede the onset of OHT or are a protective response to elevated IOP.

## *Acknowledgments*

Supported by Seoul National University Bundang Hospital Research Fund (no. 02-2016-023). The funders had no role in the design or conduct of this research. The authors alone are responsible for the content and writing of the article.

Disclosure: **J.-A. Kim,** None; **T.-W. Kim,** None; **E.J. Lee,** None; **M.J.A. Girard,** None; **J.M. Mari,** None

## *References*

1. Gordon MO, Beiser JA, Brandt JD, et al. The Ocular Hypertension Treatment Study: baseline factors that predict the onset of primary open-angle glaucoma. *Arch Ophthalmol*. 2002;120:714–720; discussion 829–730.
2. The Advanced Glaucoma Intervention Study (AGIS): 7. The relationship between control of intraocular pressure and visual field deterioration. The AGIS Investigators. *Am J Ophthalmol*. 2000;130:429–440.
3. Leske MC, Heijl A, Hussein M, et al. Factors for glaucoma progression and the effect of treatment: the early manifest glaucoma trial. *Arch Ophthalmol*. 2003;121:48–56.
4. Iwase A, Suzuki Y, Araie M, et al. The prevalence of primary open-angle glaucoma in Japanese: the Tajimi Study. *Ophthalmology*. 2004;111:1641–1648.
5. Kim CS, Seong GJ, Lee NH, Song KC; Namil Study Group, Korean Glaucoma Society. Prevalence of primary open-angle glaucoma in central South Korea the Namil study. *Ophthalmology*. 2011;118:1024–1030.
6. Kass MA, Heuer DK, Higginbotham EJ, et al. The Ocular Hypertension Treatment Study: a randomized trial determines that topical ocular hypotensive medication delays or prevents the onset of primary open-angle glaucoma. *Arch Ophthalmol*. 2002;120:701–713; discussion 829–730.
7. Quigley HA, Addicks EM, Green WR, Maumenee AE. Optic nerve damage in human glaucoma. II. The site of injury and susceptibility to damage. *Arch Ophthalmol*. 1981;99:635–649.
8. Quigley H, Anderson DR. The dynamics and location of axonal transport blockade by acute intraocular pressure elevation in primate optic nerve. *Invest Ophthalmol*. 1976;15:606–616.
9. Gaasterland D, Tanishima T, Kuwabara T. Axoplasmic flow during chronic experimental glaucoma. 1. Light and electron microscopic studies of the monkey optic nervehead during development of glaucomatous cupping. *Invest Ophthalmol Vis Sci*. 1978;17:838–846.
10. Bellezza AJ, Rintalan CJ, Thompson HW, Downs JC, Hart RT, Burgoyne CF. Deformation of the lamina cribrosa and anterior scleral canal wall in early experimental glaucoma. *Invest Ophthalmol Vis Sci*. 2003;44:623–637.
11. Yang H, Downs JC, Bellezza A, Thompson H, Burgoyne CF. 3-D histomorphometry of the normal and early glaucomatous monkey optic nerve head: prelaminar neural tissues and cupping. *Invest Ophthalmol Vis Sci*. 2007;48:5068–5084.
12. Strouthidis NG, Fortune B, Yang H, Sigal IA, Burgoyne CF. Longitudinal change detected by spectral domain optical coherence tomography in the optic nerve head and peripapillary retina in experimental glaucoma. *Invest Ophthalmol Vis Sci*. 2011;52:1206–1219.
13. Yan DB, Coloma FM, Metheetrairut A, Trope GE, Heathcote JG, Ethier CR. Deformation of the lamina

cribrosa by elevated intraocular pressure. *Br J Ophthalmol*. 1994;78:643–648.
14. Ing E, Ivers KM, Yang H, et al. Cupping in the monkey optic nerve transection model consists of prelaminar tissue thinning in the absence of posterior laminar deformation. *Invest Ophthalmol Vis Sci*. 2016;57:2914–2927.
15. Weinreb RN, Aung T, Medeiros FA. The pathophysiology and treatment of glaucoma: a review. *JAMA*. 2014;311:1901–1911.
16. Jonas JB, Aung T, Bourne RR, Bron AM, Ritch R, Panda-Jonas S. Glaucoma. *Lancet*. 2017;390:2183–2193.
17. Han JC, Choi DY, Kwun YK, Suh W, Kee C. Evaluation of lamina cribrosa thickness and depth in ocular hypertension. *Jpn J Ophthalmol*. 2016;60:14–19.
18. Yang H, Downs JC, Girkin C, et al. 3-D histomorphometry of the normal and early glaucomatous monkey optic nerve head: lamina cribrosa and peripapillary scleral position and thickness. *Invest Ophthalmol Vis Sci*. 2007;48:4597–4607.
19. Yang H, Downs JC, Burgoyne CF. Physiologic intereye differences in monkey optic nerve head architecture and their relation to changes in early experimental glaucoma. *Invest Ophthalmol Vis Sci*. 2009;50:224–234.
20. Lee EJ, Kim TW, Weinreb RN, Park KH, Kim SH, Kim DM. Visualization of the lamina cribrosa using enhanced depth imaging spectral-domain optical coherence tomography. *Am J Ophthalmol*. 2011;152:87–95.e81.
21. Girard MJ, Tun TA, Husain R, et al. Lamina cribrosa visibility using optical coherence tomography: comparison of devices and effects of image enhancement techniques. *Invest Ophthalmol Vis Sci*. 2015;56:865–874.
22. Girard MJ, Strouthidis NG, Ethier CR, Mari JM. Shadow removal and contrast enhancement in optical coherence tomography images of the human optic nerve head. *Invest Ophthalmol Vis Sci*. 2011;52:7738–7748.
23. Mari JM, Strouthidis NG, Park SC, Girard MJ. Enhancement of lamina cribrosa visibility in optical coherence tomography images using adaptive compensation. *Invest Ophthalmol Vis Sci*. 2013;54:2238–2247.
24. Lee SH, Kim TW, Lee EJ, Girard MJ, Mari JM. Diagnostic power of lamina cribrosa depth and curvature in glaucoma. *Invest Ophthalmol Vis Sci*. 2017;58:755–762.
25. Lee E, Kim T, Kim H, Lee S, Girard MJA, Mari JM. Comparison between lamina cribrosa depth and curvature as a predictor of progressive retinal nerve fiber layer thinning in primary open-angle glaucoma. *Ophthalmol Glaucoma*. 2018;1:44–51.
26. Kim JA, Kim TW, Weinreb RN, Lee EJ, Girard MJA, Mari JM. Lamina cribrosa morphology predicts progressive retinal nerve fiber layer loss in eyes with suspected glaucoma. *Sci Rep*. 2018;8:738.
27. Kim JA, Kim TW, Lee EJ, Girard MJA, Mari JM. Lamina cribrosa morphology in glaucomatous eyes with hemifield defect in a Korean population. *Ophthalmology*. 2019;126:692–701.
28. Lee EJ, Kim TW, Weinreb RN. Improved reproducibility in measuring the laminar thickness on enhanced depth imaging SD-OCT images using maximum intensity projection. *Invest Ophthalmol Vis Sci*. 2012;53:7576–7582.
29. He L, Yang H, Gardiner SK, et al. Longitudinal detection of optic nerve head changes by spectral domain optical coherence tomography in early experimental glaucoma. *Invest Ophthalmol Vis Sci*. 2014;55:574–586.
30. Roberts MD, Grau V, Grimm J, et al. Remodeling of the connective tissue microarchitecture of the lamina cribrosa in early experimental glaucoma. *Invest Ophthalmol Vis Sci*. 2009;50:681–690.
31. Lee SH, Yu DA, Kim TW, Lee EJ, Girard MJ, Mari JM. Reduction of the lamina cribrosa curvature after trabeculectomy in glaucoma. *Invest Ophthalmol Vis Sci*. 2016;57:5006–5014.
32. Jonas JB, Berenshtein E, Holbach L. Anatomic relationship between lamina cribrosa, intraocular space, and cerebrospinal fluid space. *Invest Ophthalmol Vis Sci*. 2003;44:5189–5195.
33. Morgan WH, Yu DY, Alder VA, et al. The correlation between cerebrospinal fluid pressure and retrolaminar tissue pressure. *Invest Ophthalmol Vis Sci*. 1998;39:1419–1428.
34. Jonas JB, Wang N, Wang YX, You QS, Yang D, Xu L. Ocular hypertension: general characteristics and estimated cerebrospinal fluid pressure. The Beijing Eye Study 2011. *PLoS One*. 2014;9:e100533.
35. Grytz R, Meschke G, Jonas JB. The collagen fibril architecture in the lamina cribrosa and peripapillary sclera predicted by a computational remodeling approach. *Biomech Model Mechanobiol*. 2011;10:371–382.
36. Yang H, Reynaud J, Lockwood H, et al. The connective tissue phenotype of glaucomatous cupping in the monkey eye: clinical and research implications. *Prog Retin Eye Res*. 2017;59:1–52.
37. Chung CW, Girard MJ, Jan NJ, Sigal IA. Use and misuse of Laplace's Law in ophthalmology. *Invest Ophthalmol Vis Sci*. 2016;57:236–245.
38. Bellezza AJ, Rintalan CJ, Thompson HW, Downs JC, Hart RT, Burgoyne CF. Anterior scleral canal geometry in pressurised (IOP 10) and non-pressurised (IOP 0) normal monkey eyes. *Br J Ophthalmol*. 2003;87:1284–1290.
39. Sigal IA, Yang H, Roberts MD, Burgoyne CF, Downs JC. IOP-induced lamina cribrosa displacement and scleral canal expansion: an analysis of factor interactions using parameterized eye-specific models. *Invest Ophthalmol Vis Sci*. 2011;52:1896–1907.
40. Girard MJ, Suh JK, Bottlang M, Burgoyne CF, Downs JC. Biomechanical changes in the sclera of monkey eyes exposed to chronic IOP elevations. *Invest Ophthalmol Vis Sci*. 2011;52:5656–5669.
41. Liu J, Roberts CJ. Influence of corneal biomechanical properties on intraocular pressure measurement: quantitative analysis. *J Cataract Refract Surg*. 2005;31:146–155.

Investigative Ophthalmology & Visual Science